

Synthesis of poly(*p*-phenylene vinylene) and derivatives via a new precursor route, the dithiocarbamate route

A. Henckens^{a,b}, I. Duyssens^b, L. Lutsen^b, D. Vanderzande^{a,b,*}, T.J. Cleij^a

^a IMO, division Chemistry, Campus Diepenbeek, Universiteit Hasselt, Agoralaan Building D, B-3590 Diepenbeek, Belgium

^b IMEC, Division IMOMECE, Universitaire Campus, Wetenschapspark 1, B-3590 Diepenbeek, Belgium

Received 4 May 2005; received in revised form 26 October 2005; accepted 1 November 2005

Available online 21 November 2005

Abstract

A new synthetic route towards poly(*para*-phenylene vinylene) (PPV) and its derivatives has been investigated. In this route, a bis-dithiocarbamate monomer is polymerized towards a dithiocarbamate precursor polymer by the addition of a strong base (LDA). The corresponding conjugated polymer is obtained via a heat treatment of the precursor polymer. This dithiocarbamate (DTC) precursor route strikes an optimal balance between several straightforward but sometimes troublesome precursor routes and the more complex sulphinyl precursor route yielding superior purity materials. The novelty lies in the fact that the monomer synthesis is not as difficult as compared to the sulphinyl route and this without losing the quality and accessibility of the precursor polymer. In the paper, the mechanism of the polymerization process is discussed and strong indications for radical as well as anionic mechanisms are presented.

© 2006 Elsevier Ltd. All rights reserved.

Keywords: Conjugated polymer; Dithiocarbamate precursor route; Synthesis

1. Introduction

Poly(*para*-phenylene vinylene)s (PPVs) and their derivatives have received much attention due to their applications in polymeric light emitting diodes (P-LEDs) [1]. More recently, the application range has been further extended towards other electronic applications such as photovoltaic cells. In this context, a substantial amount of research has been performed on the use of MEH-PPV [2,3] and OC₁C₁₀-PPV or MDMO-PPV [4,5] as the p-type material in the active layer of an organic solar cell. The synthesis of these conjugated materials can be performed using a variety of methods. Especially the use of precursor routes, in which a soluble precursor polymer is formed, is a viable option to introduce sufficient processability. This processability is essential for the successful incorporation of the conjugated polymer into devices. Although in some cases processability can be achieved by the introduction of solubilizing side chains, unfortunately this is not always possible, especially not for applications in which complex

functionalized materials are required. An example presented in this study is OC₈C₈-PPV which displays interesting properties for application in photovoltaic cells [6], but is insoluble in common solvents [7]. An additional advantage of the use of a precursor route is the ease in which the aromatic system can be tailored to specific needs without major adjustments to the synthetic procedures. Four precursor routes towards PPV are known, the Wessling–Zimmerman [8], the Gilch [9], the sulphinyl [10–12] and the xanthate [13] precursor route. In all these precursor polymerization routes, the actual monomer (the *p*-quinodimethane system) is always formed in situ by the addition of a base. After polymerization a soluble precursor polymer is formed, which subsequently can be converted to the conjugated system.

Recently, we reported on a new precursor route: the dithiocarbamate (DTC) route for the synthesis of PTV and its derivatives [14,15]. With this new route, the problems inherent to the Wessling–Zimmerman and Gilch precursor route such as, side reactions, instability of the precursor resulting in gelation, a limited solubility of the precursor polymer and early elimination are excluded. In addition, the high polydispersities that are observed for the precursor polymers obtained via the xanthate route are not observed for the precursors obtained via the new DTC route. Furthermore, a monomer synthesis has been developed, which is substantially more straightforward than the synthesis of the sulphinyl monomer. As a result,

* Corresponding author. Address: IMO, division Chemistry, Campus Diepenbeek, Universiteit Hasselt, Agoralaan Building D, B-3590 Diepenbeek, Belgium. Tel.: +32 11 26 83 21; fax: +32 11 26 83 01.

E-mail address: dirk.vanderzande@uhasselt.be (D. Vanderzande).

polymers (viz. monomers) that are otherwise not readily accessible, potentially can be synthesized via this route. Hence, our novel DTC route strikes an optimal balance between several straightforward but sometimes troublesome precursor routes (i.e. the Wessling–Zimmerman and Gilch routes) and rather complex precursor routes yielding superior purity materials (i.e. the sulphonyl route).

In this paper, a comparison of the DTC route with the existing precursor routes is made. In this study, PPV is chosen as a suitable model. In addition, the polymerization behavior of a selection of substituted derivatives of PPV is presented, further supporting the versatility of the DTC route.

2. Experimental section

2.1. General

Unless otherwise stated, all reagents and chemicals were obtained from commercial sources (Acros and Aldrich) and used without further purification. Tetrahydrofuran (THF) was purified by distillation from sodium/benzophenone.

NMR spectra were recorded at 300 MHz for ^1H NMR and 75 MHz for ^{13}C NMR. Gas chromatography/mass spectrometry (GC/MS) analyses were carried out with TSQ-70 and Voyager mass spectrometers (Thermoquest); the capillary column was a Chrompack Cpsil5CB or Cpsil8CB. The molecular weights and molecular weight distributions were determined relative to polystyrene standards (Polymer Labs) by size exclusion chromatography (SEC). Chromatograms were recorded on a Spectra series P100 (Spectra Physics) equipped with two Mixed-B columns (10 μm , 2 cm \times 30 cm, Polymer Labs) and a refractive index (RI) detector (Shodex) at 70 $^\circ\text{C}$. A DMF solution of oxalic acid (1.1×10^{-3} M) or THF was used as eluents at a flow rate of 1 mL/min. Fourier transform-infrared (FT-IR) spectroscopy was performed on a Perkin–Elmer Spectrum One FT-IR spectrometer (nominal resolution 4 cm^{-1} , summation of 16 scans). UV–vis spectroscopy was performed on a VARIAN CARY 500 UV–vis-NIR spectrophotometer (scan rate: 600 nm/min). Samples for temperature dependent thin film FT-IR and UV–vis characterization were prepared by spin-coating the precursor polymer from a CHCl_3 solution (10 mg/mL) onto NaCl disks at 500 rpm or quartz disks at 700 rpm. The disks were heated in a Harrick high temperature cell (heating rate: 2 $^\circ\text{C}/\text{min}$), which was positioned in the beam of either the FT-IR or the UV–vis spectrometer to allow in situ measurements. Spectra were taken continuously under a continuous flow of N_2 during which the samples were in direct contact with the heating element. Fluorescence spectra were obtained with a Perkin Elmer LS-5B luminescence spectrometer.

2.2. Synthesis of monomers

2.2.1. *p*-Xylylene bis(*N,N*-diethyl dithiocarbamate) **3a**

Monomer **3a** was prepared using two different routes (i and ii).

- (i) To 50 mL of an acetonitrile/water solution (5 vol% water) of 1,4-bis(tetrahydrothiopheno-methyl)xylylene dichloride **2a** (6 g, 17.143 mmol), sodium diethyldithiocarbamate trihydrate (or diethyldithiocarbamic acid sodium salt trihydrate) (8.87 g, 39.429 mmol) was added as a solid after which the mixture was stirred at ambient temperature for 2 h. Subsequently, water was added and the desired monomer was extracted with ether (3 \times 100 mL) and dried over MgSO_4 . Evaporation of the solvent gave 6.2 g (90% yield) of the pure product as a white solid.
- (ii) To 50 mL of an ethanol solution of α,α' -dichloro-*p*-xylylene **1a** (20 g, 0.11494 mol), sodium diethyldithiocarbamate trihydrate (59.5 g, 0.26437 mol) was added as a solid after which the mixture was stirred at ambient temperature for 2 h. Subsequently, water was added and the desired monomer was extracted with CHCl_3 (3 \times 200 mL) and dried over MgSO_4 . Evaporation of the solvent and recrystallisation from ethanol gave 45 g (98% yield) of the pure product as a white solid; mp: 78.5–79.0 $^\circ\text{C}$; ^1H NMR (CDCl_3): 7.31 (s, 4H), 4.49 (s, 4H), 4.01 (q, $J=7.2$ Hz, 4H), 3.69 (q, $J=7.2$ Hz, 4H), 1.26 (2t, $J=7.2$ Hz, 12H); ^{13}C NMR (CDCl_3): 195.10, 135.27, 129.57, 49.46, 46.70, 41.79, 12.44, 11.56; MS (EI, *m/e*): 253 ($\text{M}^+ - \text{SC}(\text{S})\text{NEt}_2$), 148 ($\text{SC}(\text{S})\text{NEt}_2$), 105 ($\text{M}^+ - 2 \times \text{SC}(\text{S})\text{NEt}_2$), 72 (NEt_2); IR (NaCl, cm^{-1}): 2974, 2931, 1486, 1416, 1268, 1208.

2.2.2. 2,5-Bis(*N,N*-diethyl dithiocarbamate-methyl)-1-(3,7-dimethyloctyloxy)-4-methoxy-benzene **3b**

The preparation is analogous to that described for **3a** (method ii). Yield: 97% (white solid); mp: 70.2–70.7 $^\circ\text{C}$; ^1H NMR (CDCl_3): 6.99 (s, 2H), 4.52 (s, 2H), 4.48 (s, 2H), 3.95 (m, 4H + 2H), 3.74 (s, 3H), 3.64 (m, 4H), 1.60–1.85 (m, 2H), 1.38–1.58 (m, 2H), 1.21 (t, 12H), 1.05–1.30 (m, 6H), 0.88 (d, 3H), 0.81 (d, 6H); ^{13}C NMR (CDCl_3): 196.11, 195.99, 151.27, 150.90, 125.08, 124.42, 114.75, 113.86, 67.13, 56.19, 49.41, 49.34, 46.61, 39.22, 37.32, 36.83, 36.30, 29.79, 27.95, 24.69, 22.69, 22.59, 19.62, 12.42, 11.59; MS (EI, *m/e*): 148 ($\text{SC}(\text{S})\text{NEt}_2$), 116 ($\text{C}(\text{S})\text{NEt}_2$); IR (NaCl, cm^{-1}): 2954, 2930, 2869, 1485, 1415, 1268, 1207.

2.2.3. 2,5-Bis(*N,N*-diethyl dithiocarbamate-methyl)-1,4-bis(octyloxy)benzene **3c**

The preparation is analogous to that described for **3a** (method ii). After purification by column chromatography (silica, hexane/ethyl acetate 9/1), the monomer was obtained as a white solid. Yield: 95%; mp: 72.5–72.8 $^\circ\text{C}$; ^1H NMR (CDCl_3): 6.99 (s, 2H), 4.54 (s, 4H), 4.02 (q, 4H), 3.91 (t, 4H), 3.69 (q, 4H), 1.73 (m, 4H), 1.42 (m, 4H), 1.18–1.36 (m, 28H), 0.86 (t, 6H); ^{13}C NMR (CDCl_3): 196.08 (2C), 150.69 (2C), 124.80 (2C), 114.66 (2C), 68.75 (2C), 49.33 (2C), 46.52 (2C), 36.84 (2C), 31.75 (2C), 29.27 (4C), 29.23 (2C), 26.07 (2C), 22.60 (2C), 14.04 (2C), 12.36 (2C), 11.55 (2C); MS (EI, *m/e*): 508 ($\text{M}^+ - \text{SC}(\text{S})\text{NEt}_2$), 148 ($\text{SC}(\text{S})\text{NEt}_2$), 116 ($\text{C}(\text{S})\text{NEt}_2$); IR (NaCl, cm^{-1}): 2928, 2855, 1485, 1414, 1268, 1204.

Table 1
Polymerization results for monomer **3a**

Entry	Polymerization temperature	Yield (%)	$M_w (\times 10^{-3})$ (DMF)	PD (DMF)
1	−78 °C	89	7.3	1.6
2	−78→0 °C ^a	88	15.0	2.1
3	0 °C	87	248.6, 11.9 ^a	1.6, 1.7 ^a
4	Room temp.	88	145.1, 7.2 ^a	1.8, 1.4 ^a

* Polymerization at −78 °C for 90 min, warming up to 0 °C for 15 min and afterwards quenching with ice water.

^a Bimodal molecular weight distribution.

2.2.4. 2,5-Bis(*N,N*-diethyl dithiocarbamate-methyl)-1,4-bis{2-[2-(2-methoxyethoxy)-ethoxy]ethoxy}benzene **3d**

The preparation is analogous to that described for **3a** (method ii). Yield: 75% (slightly yellow solid); Mp: 51.9–52.5 °C; ¹H NMR (CDCl₃): 7.01 (s, 2H), 4.54 (s, 4H), 4.09 (t, 4H), 3.81 (t, 4H), 3.60–3.76 (m, 20H), 3.53 (m, 4H), 3.36 (s, 6H), 1.25 (t, 12H); ¹³C NMR (CDCl₃): 195.80, 150.73, 125.30, 115.22, 71.84, 70.83, 70.63, 70.47, 69.69, 68.81, 58.95, 49.38, 46.56, 36.48, 12.41, 11.57; DIP MS (CI, *m/e*): 725 (M⁺), 576 (M⁺ − SC(S)NET₂); IR (NaCl, cm^{−1}): 2874, 2873, 1487, 1416, 1269, 1204.

2.3. Synthesis of precursor polymers

2.3.1. Polymerization of **3a** (**4a**)

In a typical procedure, a solution of monomer **3a** (500 mg, 1.25 mmol) in dry THF (6.25 mL, 0.2 M) was brought to a specific temperature (cf. Tables 1 and 2) and degassed for 1 h by passing through a continuous nitrogen flow. An equimolar LDA solution (625 μL of a 2 M solution in THF/*n*-heptane) was added in one go to the stirred monomer solution. The mixture was kept at the specific polymerization temperature for 90 min and the passing of nitrogen was continued. After this, the workup was dependent on the polymerization temperature employed. Polymerizations performed at −78 °C were either quenched with ethanol (6 mL) to stop the reaction (cf. Table 1, entry 1) or were allowed to come to 0 °C (cf. Table 1, entry 2). This step was not necessary if the polymerization was performed at higher temperature. The reaction mixture was quenched in ice water (100 mL), after which it was neutralized with HCl (1 M in H₂O). Subsequently, the aqueous phase was

extracted with CHCl₃ (3×60 mL). The organic layers were combined after which the solvents were removed by evaporation under reduced pressure. The resulting crude polymer was redissolved in CHCl₃ (2 mL) and a precipitation was performed in a 1/1 mixture (100 mL) of diethyl ether and hexane at 0 °C (the precipitation of polymer **4b,c,d** was performed in a 100 mL of methanol at 0 °C). The polymer was collected and dried in vacuo. The residual fractions only contained monomer residues. The yields are presented in Tables 1 and 2.

Characterization **4a–4d**: **4a**: ¹H NMR (CDCl₃): 6.78–7.14 (br s, 4H), 5.00–5.30 (br s, 1H), 3.82–4.10 (br s, 2H), 3.51–3.78 (br s, 2H), 2.92–3.12 (br s, 2H), 1.04–1.34 (br t, 6H); ¹³C NMR (CDCl₃): 194.38, 138.07, 137.17, 129.35, 128.30, 56.92, 49.15, 46.68, 42.63, 12.58, 11.65; IR (NaCl, cm^{−1}): 2978, 2931, 1486, 1414, 1266, 1205, 1141. **4b**: ¹H NMR (CDCl₃): 6.45–6.97 (br m, 2H), 5.50–5.87 (br s, 1H), 3.05–4.23 (br m, 11H), 1.02–1.95 (br m, 16H), 0.74–1.02 (m, 9H); ¹³C NMR (CDCl₃): 195.76, 150.85 (2C), 127.68 (2C), 114.11, 113.09, 67.10, 56.39, 51.98, 49.08, 46.38, 39.27, 37.54, 36.60, 34.45, 29.91, 27.92, 24.67, 22.69, 22.58, 19.66, 12.47, 11.55; IR (NaCl, cm^{−1}): 2953, 2929, 1504, 1484, 1462, 1413, 1267, 1210, 1140, 1041. **4c**: ¹H NMR (CDCl₃): 6.51–7.04 (br m, 2H), 5.52–5.84 (br m, 1H), 3.45–4.12 (br m, 8H), 3.12–3.45 (br s, 2H), 1.58–1.82 (br s, 4H), 1.01–1.55 (br m, 26H), 0.77–0.94 (br s, 6H); ¹³C NMR (CDCl₃): 196.27, 150.43 (2C), 127.73 (2C), 114.76, 113.36, 68.86 (2C), 52.11, 49.05, 46.36, 34.17, 31.93 (2C), 29.66 (4C), 29.40 (2C), 26.41, 26.28, 22.71 (2C), 14.11 (2C), 12.52, 11.64; IR (NaCl, cm^{−1}): 2927, 2855, 1503, 1484, 1413, 1267, 1209, 1141, 1010. **4d**: ¹H NMR (CDCl₃): 6.68–6.86 (br m, 2H), 5.57–5.75 (br m, 1H), 3.40–4.15 (br

Table 2
Polymerization results for monomer **3b** (entry 5–8), **3c** (entry 9–12) and **3d** (entry 13–15)

Entry	Polymerization temperature	Yield (%)	$M_w (\times 10^{-3})$ (THF)	PD (THF)
5	−78 °C	14	4.2	1.3
6	Room temp.	59	897.3, 9.5 ^a	3.3, 1.5 ^a
7	35 °C	62	386.8, 9.0 ^a	2.8, 1.5 ^a
8	65 °C	39	309.1, 1.8 ^a	3.6, 1.6 ^a
9	−78 °C	0	–	–
10	0 °C	64	1039.0, 3.3 ^a	4.3, 1.4 ^a
11	Room temp.	78	855.3, 2.0 ^a	3.6, 1.7 ^a
12	35 °C	79	303.5, 1.8 ^a	2.5, 1.6 ^a
13	−78 °C	0	–	–
14	0 °C	0	–	–
15	Room temp.	58	7.6	1.3

^a Bimodal molecular weight distribution.

m, 30H), 3.31 (br s, 6H), 1.14 (br s, 6H); IR (NaCl, cm^{-1}): 2930, 2874, 1501, 1485, 1458, 1414, 1354, 1268, 1206, 1183, 1107.

2.4. Thermal conversion of precursor polymers to conjugated polymers

Conversion of polymers **4a–4d** into the corresponding conjugated structures **5a–5d** was performed in a thin film (experimental details vide supra). In addition, the conversion of **4b** to **5b** was also performed in solution as a proof of principle. To this end, a solution of **4b** (50 mg, 0.114 mmol) in 1,2-dichlorobenzene (6 mL) was heated to 175 °C and stirred for 3 h. After removing the solvent under reduced pressure, the polymer was redissolved in CHCl_3 (1 mL) and the resulting solution was precipitated dropwise in methanol (50 mL). The polymer was filtered off and dried at room temperature under reduced pressure. Polymer **5b** was obtained as a red solid. Yield: 88%.

2.4.1. Characterization 5a–5d

5a: IR (NaCl, cm^{-1}): 1512, 1414, 1099, 960, 834. **5b**: ^1H NMR (CDCl_3): 7.5 (br, 2H), 7.2 (br, 2H), 4.6–3.2 (br m, 5H), 2.1–0.6 (br m, 19H); ^{13}C MR (CDCl_3): 151.4 (2C), 127.0 (2C), 123.3 (2C), 110.5, 108.8, 67.9, 56.4, 39.2, 37.4, 36.6, 30.2, 27.9, 24.6, 22.6 (2C), 19.8; IR (NaCl, cm^{-1}): 2954, 2871, 1497, 1463, 1409, 1244, 1202, 1033, 967, 862. **5c**: IR (NaCl, cm^{-1}): 2928, 2858, 1496, 1411, 1378, 1200, 1141, 1041, 968. **5d**: IR (NaCl, cm^{-1}): 2935, 2874, 1498, 1192, 1108, 965.

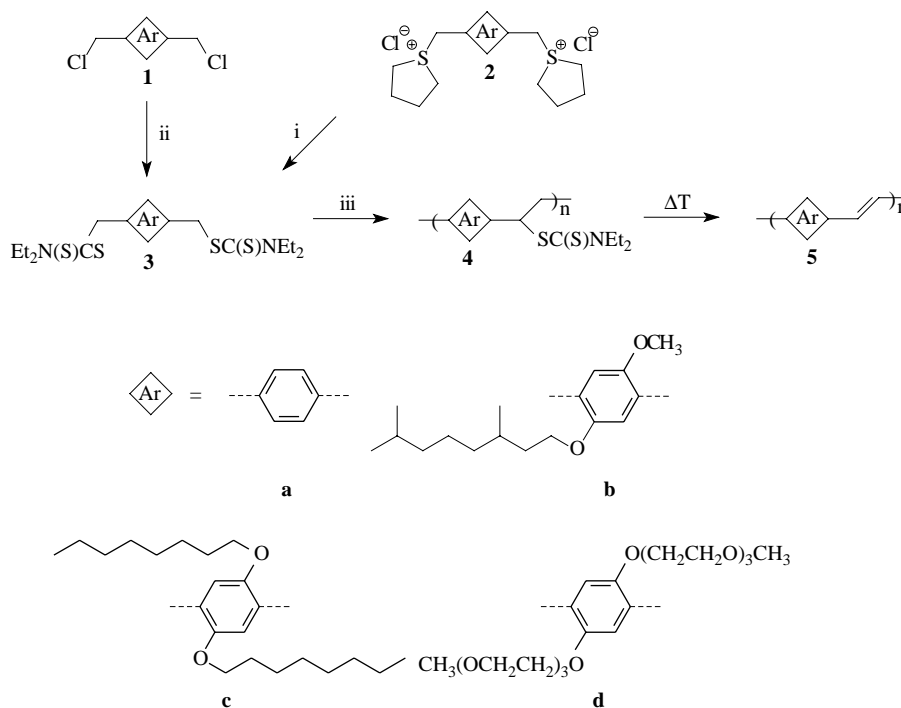
3. Results and discussion

3.1. Synthesis of the dithiocarbamate precursor of PPV and its conversion

3.1.1. Mechanistical aspects of the polymerization: competition anionic/radical?

To study the polymerization process via the dithiocarbamate route, *p*-xylylene bis(*N,N*-diethyl dithiocarbamate) **3a** was synthesized. This was accomplished by the addition of sodium diethyldithiocarbamate trihydrate either to the bisulphonium salt **2a** (Scheme 1, step i) or to α - α' -dichloro-*p*-xylene **1a** (Scheme 1, step ii). The latter pathway is straightforward and provides superior yields and, hence, was also used for preparation of several other monomers (vide infra). The bis-dithiocarbamate monomer **3a** was polymerized and the results of these polymerizations are presented in Table 1.

Lithium diisopropyl amide (LDA) was used as the base, dried THF as the solvent and the monomer concentration was set at 0.2 M. All polymerization reactions were terminated after 90 min. The influence of the temperature was verified by using four different polymerization temperatures (ranging from -78 °C to room temperature, cf. Table 1 entries 1–4). From the data in Table 1 it can be concluded that by using the new dithiocarbamate precursor route, it is possible to obtain the precursor polymer in an excellent yield for all applied temperatures. Molecular weights were determined by GPC relative to polystyrene (PS) standards with DMF as the eluent, which is a good solvent for precursor polymer **4a**. The obtained molecular weight distributions are mono- or bimodal with weight-average molecular weights ranging from 7300 to 248600 g/mol, dependent on the temperature employed.



Scheme 1. Synthesis of the monomers and polymers. (i) $\text{NaSC(S)NEt}_2 \cdot 3\text{H}_2\text{O}$, (ii) $\text{NaSC(S)NEt}_2 \cdot 3\text{H}_2\text{O}$, (iii) LDA.

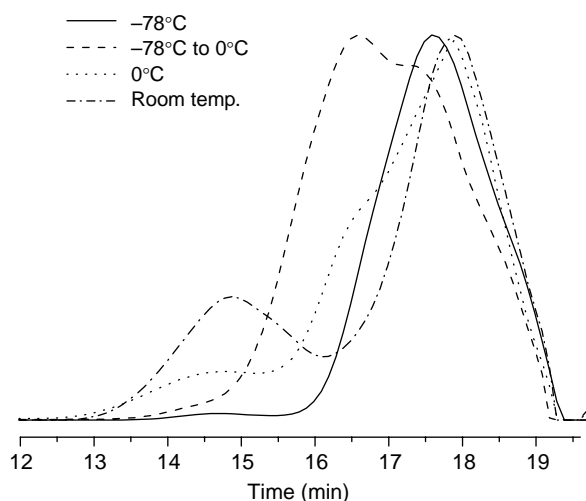


Fig. 1. Overlay of GPC-chromatograms (DMF) of precursor polymer **4a** synthesized at different temperatures.

The molecular weights of the precursor polymers **4a** were in general lower than those of the xanthate precursor polymers obtained under similar polymerization conditions [13,16] and the sulphinyl precursor polymers [17].

To demonstrate the effect of temperature on the molecular weights, an overlay of the chromatograms of the four different entries is presented in Fig. 1. The chromatogram of precursor polymer **4a** prepared at $-78\text{ }^{\circ}\text{C}$ (solid line) shows a monomodal molecular weight distribution. As the polymerization temperature is increased an additional distribution at the high molecular weight side of the chromatogram becomes apparent and a bimodal molecular weight distribution is observed.

In previous studies, we also observed a bimodal molecular weight distribution for the PPV precursors obtained via the sulphinyl precursor route [11]. It was proven that the high molecular weight fraction was formed via a radical polymerization mechanism and that an anionic mechanism was responsible for the formation of the low molecular weight polymer [18]. Further research has corroborated these earlier findings and indicates that the occurrence of simultaneous mechanisms is not unexpected for the polymerization behavior of *p*-quinodimethane systems [19]. However, a full discussion on the polymerization mechanisms of *p*-quinodimethane systems in general is beyond the scope of this paper.

To verify whether a similar explanation is valid for the DTC precursor route, the effect of the addition of a radical inhibitor, 2,2,6,6-tetramethylpiperinoxyl (TEMPO), was studied. To this end 0.5 equiv TEMPO was added to the polymerization mixture. It was observed that the addition of the radical scavenger inhibited the formation of the high molecular weight polymer (Fig. 2).

The fact that 0.5 equiv TEMPO inhibits the polymerization reaction was already proven in a broad range of solvents for the sulphinyl precursor route. In MMF and *s*-BuOH for example, the polymerization was almost completely inhibited [17,20] and in NMP, a dipolar, aprotic solvent in which a bimodal molecular weight distribution could be observed, the formation

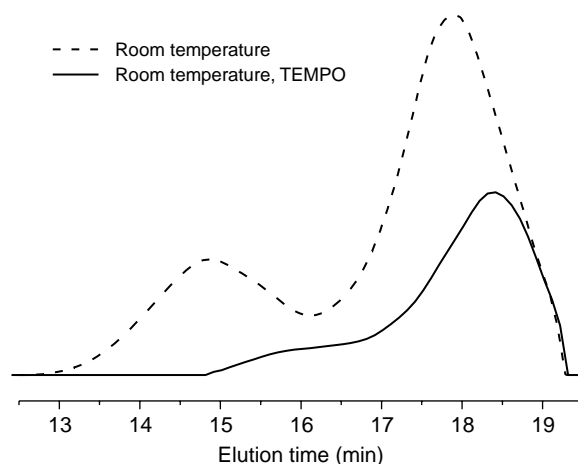


Fig. 2. Overlay of GPC-chromatograms (DMF) of precursor polymer **4a** synthesized at room temperature with or without added TEMPO.

of high molecular weight sulphinyl precursor polymers was inhibited [18]. The experiment with the addition of TEMPO to the reaction of **3a** with LDA (solvent THF) indeed suggests that in the DTC precursor route a similar mechanism is present as was observed for the sulphinyl precursor route.

This conclusion is corroborated by additional polymerization experiments of monomers with poly(oxyethylene) (PEO) side chains. The introduction of PEO side chains could eventually lead to water-soluble polymers. The polymerization results obtained for the PEO monomer **3d** (Table 2, entries 13–15) indicate that when the polymerization temperature is low, no polymer could be isolated. Only at higher temperature a polymer fraction is observed in the GPC chromatogram. This is consistent with the fact that the PEO side chains are rather hygroscopic making it difficult to work under completely dry conditions. As a result, traces of water present in the polymerization mixture will kill the base and, therefore, inhibit the anionic mechanism. Since at low temperature no radical polymerization can occur, no polymer has been formed.

It is noteworthy that attempts to polymerize **3a** with less strong bases like NaOtBu and NaH did not lead to polymer **4a**. Also the use of *n*-BuLi as the base was unsuccessful to obtain polymer. After work-up, no precipitate was formed in methanol and the monomer could be fully recuperated. This indicates the necessity of a strong base like LDA in the DTC precursor route.

3.1.2. Conversion of the precursor **4a** towards PPV **5a**

The thermal conversion to the conjugated structure has been studied by means of in situ UV–vis and FT-IR spectroscopy during which the spin-coated precursor polymer is heated at $2\text{ }^{\circ}\text{C}/\text{min}$ from ambient temperature up to $350\text{ }^{\circ}\text{C}$ under a continuous flow of N_2 . The absorption maximum (λ_{max}) of 406 nm at $270\text{ }^{\circ}\text{C}$ for the PPV prepared via the dithiocarbamate precursor route (Fig. 3) is shifted to longer wavelength (lower energy) compared to the value of 396 nm [16] at $270\text{ }^{\circ}\text{C}$ obtained by the precursors prepared via the xanthate route. This is an indication of a significantly improved conjugation of the π -electron system.

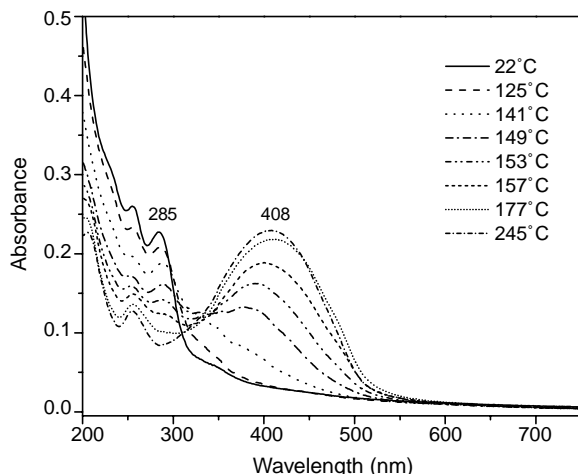


Fig. 3. UV-vis spectra of **4a** at different temperatures.

As already stated, the λ_{max} value of 406 nm for the PPV prepared using the DTC route is measured at high temperature. The value at room temperature is shifted bathochromically due to the thermochromic effect [21]. The room temperature absorption maximum of the PPV from the dithiocarbamate precursor is 420 nm (Table 3; a red shift of 14 nm as compared to the λ_{max} value at 270 °C is observed). However, in comparison with the PPV obtained from the *n*-butyl-sulphinyl precursor polymer (λ_{max} 425 nm at room temperature, λ_{max} 416 nm at 120 °C) [21], the λ_{max} is somewhat shifted to shorter wavelength. Hence, a slightly better conjugated system for the PPV obtained from the *n*-butyl-sulphinyl precursor polymer is observed as compared to the PPV obtained from the diethyl DTC precursor. Notwithstanding, the optical properties of the PPV obtained using the DTC route are significantly better than those obtained using most other synthetic procedures. In addition to λ_{max} , also the optical band gap was determined from the UV-vis spectroscopy data. An optical band gap of 2.37 eV was determined from the low energy edge of the π - π^* absorption band which is similar to the value reported by other researchers [22].

The absorbance at the absorption maximum of both dithiocarbamate precursor **4a** and PPV **5a** are plotted as a function of increasing temperature in Fig. 4. From these profiles, it can be seen that the elimination of the dithiocarbamate groups of the precursor starts at about 115 °C and is completed around 170 °C under these heating conditions. The elimination takes place in the same temperature regime as was found for the conversion of the thiophene dithiocarbamate precursor towards PTV [14]. Notwithstanding, the temperature on which the elimination starts is lower compared to the

Table 3

Absorption maxima of the conjugated polymers **5** obtained after elimination in film of the precursor polymers **4**

Polymer	λ_{max} (nm) at high temperature	λ_{max} (nm) at room temperature
5a	406 (270 °C)	420
5b	465 (160 °C)	510
5c	480 (177 °C)	495
5d	453 (163 °C)	464

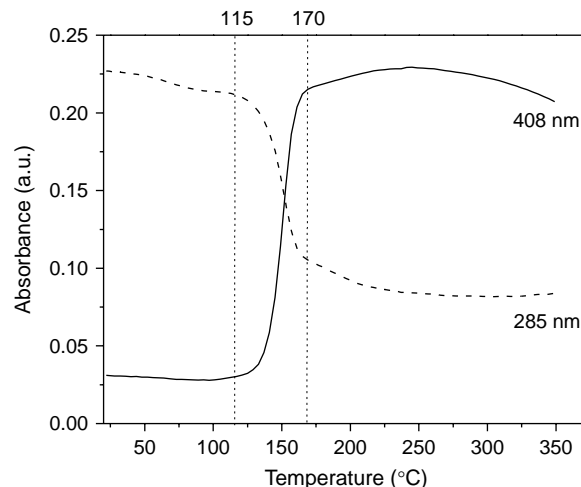


Fig. 4. Absorbance profiles at 285 and 408 nm as a function of temperature for **4a**.

xanthate precursor route (150 °C) [16] and much higher compared to the start of the elimination of the *n*-butyl-sulphinyl group (circa 65 °C) [21].

The temperature dependent IR spectra of the conversion process of precursor polymer **4a** obtained using in situ FT-IR spectroscopy are shown in Fig. 5. In the IR spectrum of **4a** strong vibrations arising from the dithiocarbamate leaving group are visible at 1486, 1414, 1266 and 1205 cm^{-1} . Upon heating polymer **4a**, the elimination of the dithiocarbamate groups is readily observed by the disappearance of these vibrations. Also a new vibration appears at 960 cm^{-1} which originates from the *trans*-vinylene double bond. The vibration at 834 cm^{-1} of the *p*-phenylene C-H out-of-plane deformation [16,23] also increases during the elimination process. Both the decline in dithiocarbamate absorption and the increase in double bond absorption start around 105 °C as visualized in Fig. 6. There is no indication for the formation of *cis* double bonds, which differs from the observations for the corresponding xanthate precursor polymer [16]. From the temperature dependent FT-IR spectral data it is also evident that after

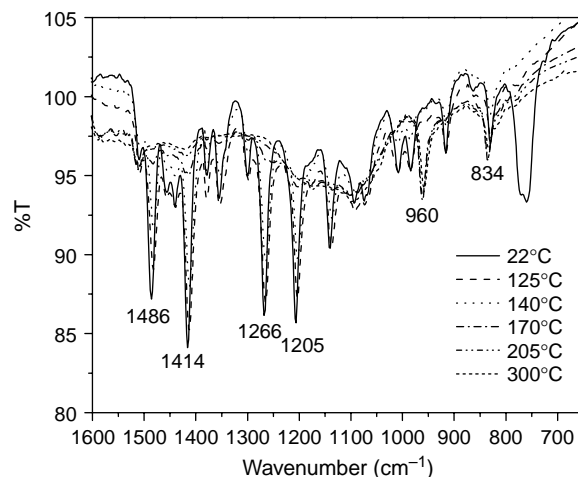


Fig. 5. IR spectra of **4a** at different temperatures.

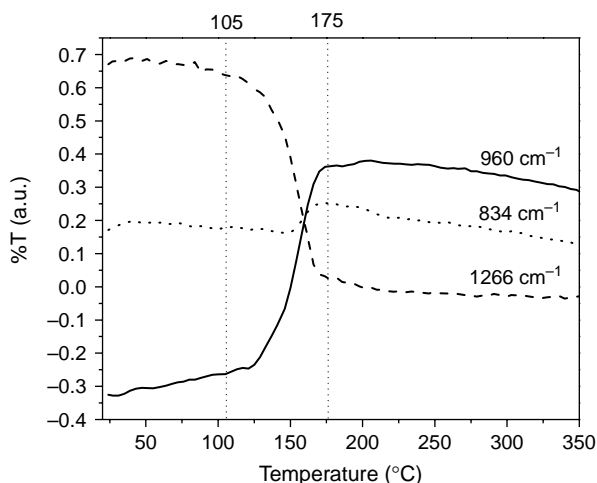


Fig. 6. IR absorption profiles at 1266, 960 and 834 cm^{-1} as a function of temperature for **4a**.

treatment above 200 °C no residual products of the thermal conversion remain.

The thermal stability of conjugated polymers is characterized by the stability of the conjugated system. Once a breakdown of conjugation occurs, a conjugated polymer is no longer suitable for opto-electronic applications. The breakdown of the conjugated system can be directly measured with in situ UV–vis and FT-IR spectroscopy. From these measurements it is evident that the conjugated backbone of PPV is stable until 350 °C. For comparison, the thermal stability of **5a**, as measured with TGA, is 538 °C.

3.2. Synthesis of the dithiocarbamate precursor of OC_1C_{10} -PPV and its conversion

3.2.1. Synthesis of the dithiocarbamate precursor

To further demonstrate the versatility of the DTC precursor route, a substituted PPV-derivative, i.e. OC_1C_{10} -PPV, was prepared. The synthesis of monomer **3b** is a single step reaction from the corresponding halogenide **1b** (Scheme 1). The polymerizations were all performed in the same way as described for the synthesis of PPV and the results are listed in Table 2 (entry 5–8). All the molecular weights of the precursor polymers were determined by means of GPC relatively to polystyrene standards in THF, which is a good solvent for this particular polymer. From Table 2 it is obvious that high molecular weight OC_1C_{10} -PPV can readily be prepared via the DTC precursor route.

Similarly to the results found for PPV, the temperature also has a pronounced effect on the molecular weights of the OC_1C_{10} precursor polymers **4b**. At low temperatures (entry 5) only low molecular weight material is formed. At room temperature also high molecular weight material is present of which the molecular weight decreases with increasing temperature. This is in agreement with our previous experiments in which it was proven that for the precursors obtained via the sulphanyl precursor route, the molecular weight decreased when the polymerization temperature was

augmented. However, whereas the molecular weight of the high molecular weight fraction decreases with increasing temperature, the relative amount of high molecular weight polymer actually increases with increasing temperature. Apparently, an increased temperature is favorable for the radical mechanism. Also here the addition of TEMPO on the polymerization was studied and the same conclusions could be drawn as for the PPV precursor, i.e. the high molecular weight fraction was reduced.

3.2.2. Conversion of precursor **4b** towards the corresponding conjugated polymer **5b**

Since the conjugated polymer has solubilising side chains, the thermal conversion was also performed in solution. Whereas a complete elimination of the *n*-butyl sulphanyl groups was observed after refluxing the sulphanyl precursor in toluene (110 °C) for 3 h, it was necessary to heat precursor **4b** in 1,2-dichlorobenzene (175 °C) for 3 h to fully eliminate the dithiocarbamate groups. It is evident from FT-IR spectroscopy that after conversion at this temperature no residual products of the thermal conversion remain. Heating the precursor **4b** in chlorobenzene (125 °C) for 25 h did not lead to a fully converted polymer according to UV–vis spectroscopy. As for an *n*-alkyl-sulphanyl OC_1C_{10} -PPV precursor polymer, also the dithiocarbamate OC_1C_{10} -PPV precursor is a sticky solid product, which turns into a red fibrous solid after the elimination. The absorption maximum (λ_{max}) of the conjugated OC_1C_{10} -PPV polymer eliminated in solution and measured in film at ambient temperature is 510 nm which is 7 nm blue shifted compared to the λ_{max} value (of 517 nm) at room temperature for the same polymer obtained from the *n*-butyl sulphanyl precursor [21]. This observation is similar to the one observed for PPV (vide supra).

In addition to the solution process, the conversion of **4b** was also followed in a thin film with in situ UV–vis and FT-IR spectroscopy. In Fig. 7, the thin film UV–vis spectra of the conversion of **4b** at different temperatures are shown. The λ_{max} values of **5b**, both at high temperature and at room temperature are listed in Table 3. It should be noted that no difference in solubility exists between **5b** prepared in solution and **5b**

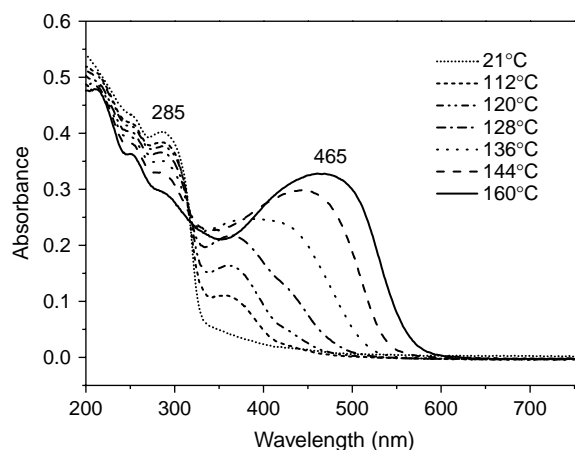


Fig. 7. UV–vis spectra of **4b** at different temperatures.

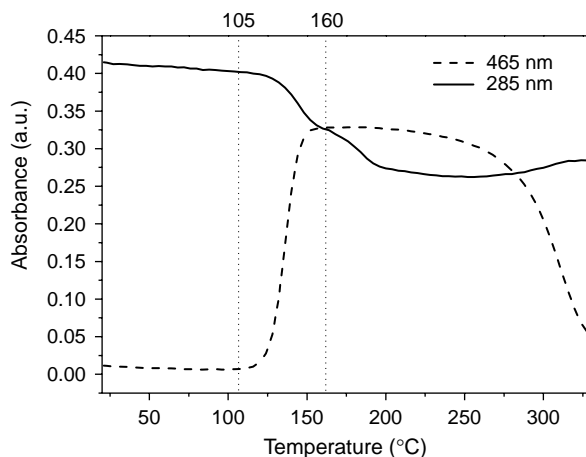


Fig. 8. Absorbance profiles at 285 and 465 nm as a function of temperature for **4b**.

converted in a thin film. Since also no differences in the UV–vis absorption characteristics are observed, it can be assumed that the nature of the conversion process has no significant effect on the final conjugated polymer properties.

From the absorbance profiles in Fig. 8, it appears that OC₁C₁₀–PPV is thermally stable until a temperature of 270 °C. This value is significantly higher than the reported value of 230 °C for the same polymer when it was made from the sulphanyl precursor [21]. Although we have to take into account that the elimination temperature of a sulphanyl group (65 °C) is lower than the one observed for the dithiocarbamate group (115 °C), this discrepancy is surprising. Therefore, an additional in situ UV–vis experiment was performed in which the precursor was eliminated in film (heating from room temperature to 180 °C), cooled back to room temperature and heated again to 350 °C. The profile of the heating after conversion is shown in Fig. 9 (solid line) and it is evident that the conjugated system is now stable until a temperature of 230 °C. Apparently the history of the sample determines to a significant degree the degradation behavior. It should be noted that the decrease in absorbance below 230 °C is a result of the thermochromic effect.

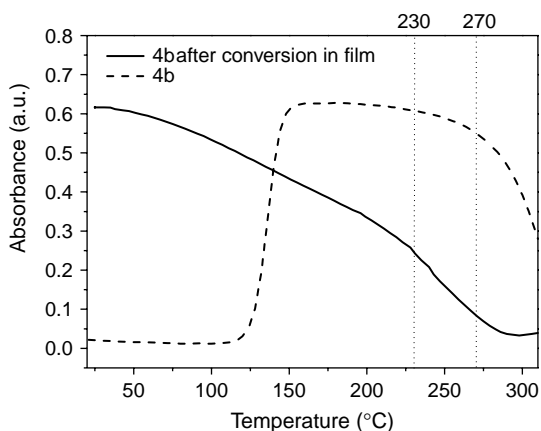


Fig. 9. Absorbance profiles for **4b** and **5b**.

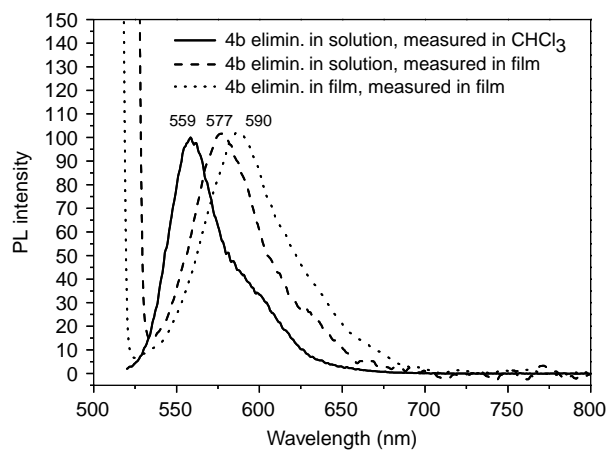


Fig. 10. PL spectra of **5b**.

The photoluminescence (PL) spectra of polymer **5b** are shown in Fig. 10. It can be seen that the method of processing the thin film influences the fluorescence properties in a similar way as was observed for OC₁C₁₀–PPV obtained from a sulphanyl precursor polymer [24]. When the conversion was performed in film (dotted line), the fluorescence emission maximum ($\lambda_{\text{max}} = 590$ nm) was red shifted compared to the maximum measured for a drop-casted film of OC₁C₁₀–PPV which was converted in solution (dashed line) ($\lambda_{\text{max}} = 577$ nm). Such differences in the fluorescence emission maximums reflect differences in morphology of the thin films. These differences are even more pronounced when comparing OC₁C₁₀–PPV obtained from a conversion in film of a DTC precursor ($\lambda_{\text{max}} = 590$ nm) with OC₁C₁₀–PPV obtained from an *n*-butyl sulphanyl precursor ($\lambda_{\text{max}} = 640$ nm). A possible explanation is that the lower defect levels in the latter result in a better packing of the polymer chains, which accounts for the red shift in the emission maximum.

3.3. Synthesis of other dithiocarbamate precursors of PPV derivatives

Besides the synthesis of the PPV and OC₁C₁₀–PPV dithiocarbamate precursors, two other substituted PPV derivatives were synthesized via the dithiocarbamate route: OC₈C₈–PPV **5c** (also sometimes referred to as DO–PPV, DOO–PPV or C₈–PPV), a derivative with linear chains and diPEO–PPV **5d**, a derivative with more polar side chains.

The polymer OC₈C₈–PPV is of interest since by introducing linear side chains, the charge carrier mobility in the conjugated polymer can possibly be improved. However, in the conjugated form OC₈C₈–PPV is insoluble which is attributed to the fact that the octyl chains are ordered. The use of a precursor route is, therefore, essential. The results of the polymerization via the dithiocarbamate precursor route are listed in Table 2 (entry 9–12). The changes in molecular weight as a function of the polymerization temperature are similar to those observed for OC₁C₁₀–PPV (vide supra). For example, the tendency that for the high molecular weight interval the observed molecular weight decreases at higher temperature is confirmed. Following

the conversion with in situ UV–vis and FT-IR leads to the conclusion that the temperature at which the elimination starts is similar to the one observed for PPV and OC₁C₁₀–PPV. The room temperature UV–vis absorption maximum λ_{max} is 495 nm (Table 3). In comparison, the maximum absorption of a film of OC₈C₈–PPV polymer obtained via the Gilch route is 490 nm [6], indicating that also for this polymer the DTC route gives better results than most of the other available precursor routes. The thermal stability of the conjugated system of **5c** is similar to that of **5b**, i.e. a thermal stability up to temperature of 225 °C. It is evident from FT-IR spectroscopy that after heating above 170 °C no residual products of the thermal conversion remain.

Finally the DTC route was also tested for monomers with PEO side chains (vide supra). The thermal conversion was again followed with in situ UV–vis. From the UV–vis measurements it is also in this case evident that the conjugated system of diPEO-PPV **5d** is stable up to 225 °C. The observed absorption maximums of **5d**, both at high (163 °C) and at room temperature are listed in Table 3. It is evident from FT-IR spectroscopy that after heating above 160 °C no residual products of the thermal conversion remain. The fact that **5d** readily can be prepared further corroborates the broad versatility of our novel DTC precursor route in the synthesis of substituted conjugated polymers.

4. Conclusion

We have synthesized various dithiocarbamate precursor polymers, which on thermal heat treatment convert into the corresponding PPV derivatives. Under most polymerization conditions tested, analytical size exclusion chromatography indicates the presence of a bimodal molecular weight distribution. There are strong indications that this is caused by the presence of a competition between radical and anionic polymerization mechanisms.

The new DTC route is an interesting synthetic alternative for three earlier reported precursor routes (Wessling, Gilch, xanthate), tackling the disadvantages associated with these routes and producing polymers of superior quality. However, it should be noted that the already existing sulphanyl route is a more robust route, which results in polymers with lower defect levels. Notwithstanding, the DTC route is a viable alternative for the sulphanyl precursor route, especially in cases where the sulphanyl monomer is difficult to synthesize.

Acknowledgements

A. Henckens wishes to thank I. Vanseveren and W. Oosterbaan for the synthesis of **1d** and **1c**, respectively,

and H. Penxten for the in situ UV–vis and FT-IR measurements. This work was financially supported by the FWO-Vlaanderen, the European Commission (project ‘EUROMAP’ HPRN-CT-2000-00127), DWTC (Services of the Prime Minister-Federal Service for Scientific, Technical and Cultural affairs; TAP-project ‘SOLTEX’ PA-07-095) and the IWT (Institute for the Promotion of Innovation by Science and Technology in Flanders) via the SBO-project 030220 ‘Nanosolar’.

References

- [1] Kraft A, Grimsdale AC, Holmes AB. *Angew Chem Int Ed* 1998;37:402–28.
- [2] Sariciftci NS, Braun D, Zhang C, Srdanov VI, Heeger AJ, Stucky G, et al. *Appl Phys Lett* 1993;62(6):585–7.
- [3] Halls JJM, Pichler K, Friend RH, Moratti SC, Holmes AB. *Appl Phys Lett* 1996;68(22):3120–2.
- [4] Munters T, Martens T, Goris L, Vrindts V, Manca JV, Lutsen L, et al. *Thin Solid Films* 2002;403:247–51.
- [5] Hoppe H, Niggemann M, Winder C, Kraut J, Hiesgen R, Hinsch A, et al. *Adv Funct Mater* 2004;14(10):1005–11.
- [6] Chen SH, Su AC, Han SR, Chen SA, Lee YZ. *Macromolecules* 2004;37(1):181–6.
- [7] Drdic C, Bleib N, Chaiebb A, Majdoub M, Roudeslib MS, Davenasa J, et al. *Eur Polym J* 2001;37(4):683–90.
- [8] Wessling RA. *J Polym Sci, Polym Symp* 1985;72:55–66.
- [9] Gilch HG, Wheelwright WL. *J Polym Sci* 1966;4:1337–49.
- [10] Louwet F, Vanderzande D, Gelan J. *Synth Met* 1992;52(1):125–30.
- [11] Louwet F, Vanderzande D, Gelan J. *Synth Met* 1995;69:509–10.
- [12] Louwet F, Vanderzande D, Gelan J, Mullens J. *Macromolecules* 1995;28:1330–1.
- [13] Son S, Dodabalapur A, Lovinger AJ, Galvin ME. *Science* 1995;269:376–8.
- [14] Henckens A, Lutsen L, Vanderzande D, Knipper M, Manca J, Aernouts T. *Proc SPIE Int Soc Opt Eng* 2004;5464:52–9.
- [15] Henckens A, Colladet K, Fourier S, Cleij TJ, Lutsen L, Gelan J, et al. *Macromolecules* 2005;38(1):19–26.
- [16] Kesters E, Gillissen S, Motmans F, Lutsen L, Vanderzande D. *Macromolecules* 2002;35(21):7902–10.
- [17] Van Breemen AJJM, Issaris ACJ, de Kok MM, Van Der Borght MJAN, Adriaensens PJ, Gelan JMJV, et al. *Macromolecules* 1999;32(18):5728–35.
- [18] Hontis L, Van Der Borght M, Vanderzande D, Gelan J. *Polymer* 1999;40:6615–7.
- [19] Vanderzande DJM, Hontis L, Palmaerts A, Van Den Berghe D, Wouters J, Lutsen L, et al. *Proc SPIE* 5937:116–125.
- [20] Issaris A, Vanderzande D, Gelan J. *Polymer* 1997;38(10):2571–4.
- [21] Kesters E, Vanderzande D, Lutsen L, Penxten H, Carleer R. *Macromolecules* 2005;38(4):1141–7.
- [22] Eckhardt H, Shacklette LW, Jen K-Y, Elsenbaumer RL. *J Chem Phys* 1989;91(2):1303–15.
- [23] Williams DH, Fleming I. *Spectroscopic methods in organic chemistry*. 5th ed. London: The McGraw-Hill Companies; 1995.
- [24] Lutsen L, Adriaensens P, Becker H, Van Breemen AJ, Vanderzande D, Gelan J. *Macromolecules* 1999;32:6517–25.